



## Ascorbic acid: $\beta$ -cyclodextrin supported greenly synthesized CuSeO<sub>4</sub> nanocomposite for catalytic degradation of organic dyes

Subbulakshmi Mariappan<sup>a</sup>, Thavuduraj Kavitha<sup>a\*</sup>, Leeladevi Karuppasamy<sup>a</sup>  
<sup>a, a\*</sup> Department of Chemistry, Sri S. Ramasamy Naidu Memorial College (Affiliated to Madurai Kamaraj University), Sattur – 626 203, Tamil Nadu, India.  
Email: mssubha85@gmail.com

### Abstract

In the present study, describe a facile synthesis of Copper selenate (CuSeO<sub>4</sub>) decorated  $\beta$ -cyclodextrin (As:  $\beta$ -CD IC/CuSeO<sub>4</sub>) nanocomposite for the utilization of photocatalytic activity, anti-oxidant activity, and antimicrobial activity. CuSeO<sub>4</sub> nanocomposites are synthesised via simple and green methods using  $\beta$ -cyclodextrin as reducing agents. When utilised as an antibacterial agent against a Gram-positive and a Gram-negative bacterium, the As:  $\beta$ -CD IC/CuSeO<sub>4</sub> nanocomposite is a remarkable material in suppressing the challenged bacterial strains. The As:  $\beta$ -CD IC/CuSeO<sub>4</sub> composite has shown exceptional activity with an 18-mm inhibitory zone at different concentrations of 50 mg/ml, 75 mg/ml, and 100 mg/ml, and maintains significant antibacterial efficacy for 72 h, proving its sustainable performance for a long-life period. The As:  $\beta$ -CD IC/CuSeO<sub>4</sub> nanocomposite effectively scavenged the 2,2-diphenyl-1-picrylhydrazyl free radical. Additionally, under UV-Visible illumination, the photocatalytic performance of As:  $\beta$ -CD IC/CuSeO<sub>4</sub> was examined for the oxidative destruction of the organic dyes methyl orange (MO) and methylene blue (MB) without the need of any harmful reducing agents. The As:  $\beta$ -CD IC/CuSeO<sub>4</sub> catalyst shows superior catalytic activity and more than 65% of efficiency.

**Keywords:** As:  $\beta$ -CD IC/CuSeO<sub>4</sub>, Green Synthesis, Photocatalytic activity, organic moiety, degradation

## **1 Introduction**

Nanocomposites are promising materials because of their unique character and enormous features in the past few decades [1-4]. There are plenty of studies are performed in various aspects such as the detection of pathogenic bacteria, gas sensors, and biomedical diagnostics [5-10]. The physical and chemical properties of bimetallic nanostructures are frequently well-defined and improved, linking the effects of the two metal components [11–14]. The production of materials with better magnetic, catalytic, and thermal properties can benefit from the use of precisely, structurally organised intermetallic nanostructures with specified stoichiometric composition and an ordered lattice structure [15–20]. Considerable attention has been rewarded to the preparation and characterization of metal chalcogenides owing to their fascinating properties and potential applications. Recently, the improper release of hazardous pollution from various chemical industries causes major threats to the environment as well as living organisms. Methylene blue (MB, cationic), indigo carmine (IC, anionic), and other organic dyes have extremely toxic by-products that are found in wastewater from a variety of industries. The organic contaminants in the wastewater are removed from the water using a variety of techniques, including ozonation, membrane separation, coagulation, and adsorption. The most effective approach, most environmentally friendly technique, and least expensive way to degrade the organic contaminant from wastewater is a photocatalytic study.

The metal selenium (Se) is a highly demanding element for a variety of applications, including glass manufacturing pigments, agricultural feed additives, chemical uses, and pharmaceuticals, according to the literature review. It is a naturally occurring element that can be found in a variety of isotropic and allotropic shapes, including hexagonal, trigonal, monoclinic, and amorphous. Parkin and Co-workers reported a route to synthesize selenides by a reaction of

Se with elemental metals in amine solutions. Despite these, the increased recombination rate of photogenerated electron-hole pairs has prevented (Se) from being fully utilised in practical photocatalysis. Numerous efforts like structural alteration, coupling with metal-free or metal elements, constructing hetero-junctions, and doping with metals have been attempted to get the enhanced photocatalytic activity of (Se). However, copper nanoparticles (Cu-NPs) possess a wide range of potential applications in nanotechnology including catalysts, lubricant additives, nanofluids for heat transfer, electronic and optical devices manufacturing, conductive inks, solar energy conversion materials, biosensors, anti-biofouling agents, and cancer cell treatments [21]. In addition to that, copper nanoparticles can be a reassuring element to replace expensive noble metal nanoparticles such as silver, gold, platinum, and palladium. The characteristics of nanoparticles of binary compounds like copper II-IV chalcogenides can be controlled by both quantum-size effects and chemical composition. The use of biomolecules such oleic acid, -cyclodextrin, and cytochrome C3 as stabilisers and ascorbic acid as a reducing agent for the synthesis of bimetallic nanostructures is becoming increasingly common in order to minimise the use of dangerous chemicals as reducing agents. Hence, we developed Copper Selenate (CuSeO<sub>4</sub>) decorated  $\beta$ -cyclodextrin, As:  $\beta$ -CD IC/CuSeO<sub>4</sub> nanocomposite [22,23].

Very few reports have been reported on the application of CuSe nanomaterials in photocatalytic activity. Herein, we chosen selected copper selenide nanocrystals (CuSe) coupled with an ascorbic acid,  $\beta$ -Cyclodextrin (stabilization agent) to prepare a simple, non-toxic, environmentally friendly Copper Selenate inclusion complex [24]. The unique needle-like structure of  $\beta$ -Cyclodextrin is more favourable for the formation of inclusion complexes with 2D inorganic crystals. Additionally, scanning electron microscopy with energy dispersion spectroscopy, X-ray diffraction analysis, and UV-visible spectroscopy were used to characterise

the as-prepared As:  $\beta$ -CD IC/CuSeO<sub>4</sub> nanocomposite. As prepared As:  $\beta$ -CD IC/CuSeO<sub>4</sub> shows unique properties and enhanced bio-compatibility. The degradation of Methylene blue (MB) and Methyl Orange (MO) dye was used to test the catalytic activity of the As:  $\beta$ -CD IC/CuSeO<sub>4</sub> nanocomposite. Besides that, the antimicrobial and antioxidant activity of as-prepared As:  $\beta$ -CD IC/CuSeO<sub>4</sub> nanocomposite was also investigated.

## 2 Materials and methods

### 2.1 Reagents

From Sigma-Aldrich, we obtained copper sulphate (CuSO<sub>4</sub>), selenium dioxide (SeO<sub>2</sub>), ascorbic acid, and  $\beta$ -cyclodextrin. None of the other compounds underwent any additional purification before use. Throughout the experiments, distilled water was utilised to create all of the necessary solutions.

### 2.2 Green Synthesis of As: $\beta$ -CD IC/CuSeO<sub>4</sub>

The aqueous solutions of Copper sulphate (CuSO<sub>4</sub>) 0.3950 g in 50 ml / Selenium dioxide (SeO<sub>2</sub>) 0.3830 g in 50 ml, Ascorbic acid (2.190 g in 50 ml), and  $\beta$  - Cyclodextrin (0.505 g in 50 ml) were prepared; the aqueous solutions of Copper and selenium were poured into a beaker, and heated at 80 °C. Then ascorbic acid and  $\beta$ -CD were added to the above solution with magnetic vigorous agitation (700 rpm). The colour of the solution changed, from light blue to light green, and finally dark violet precipitate began. The reaction conditions were maintained for 5 h and then cooled to room temperature. After that, the solution with the dark violet precipitate was centrifuged for 10 min at 4000 rpm. The precipitate was washed with distilled water and ethanol. Finally, the precipitate was dried at room temperature to obtain the As:  $\beta$ -CD IC/CuSeO<sub>4</sub>.

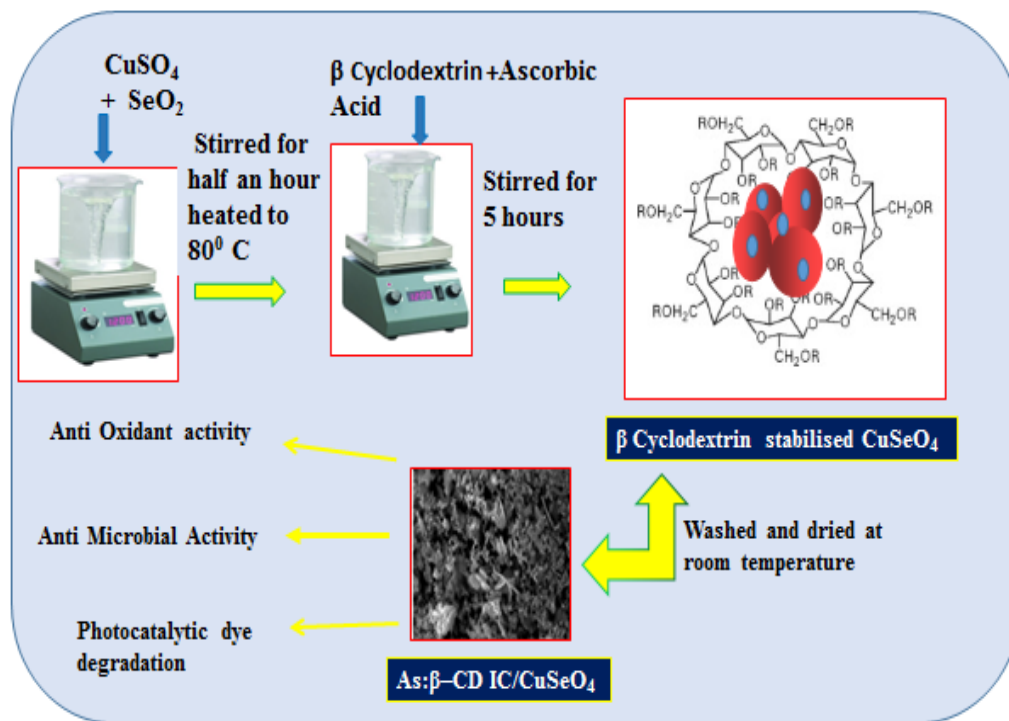


Fig 1: Schematic representation of biosynthesis of As:  $\beta$ -CDIC/ $\text{CuSeO}_4$

### 2.3 Characterization of photocatalyst

Using a Bruker D2 diffractometer at 40 kV and 25 mA, the crystalline structure of as-produced nanoparticles was examined. The measurements were taken with the secondary graphite monochromatic Cu K alpha radiation ( $\lambda=1.54060\text{\AA}$ ), and the scan speed was  $0.02^\circ$ . The measurements were taken at a high angle of  $2\theta$  in the range of  $5^\circ$ - $80^\circ$ . The formation of As:  $\beta$ -CD IC/ $\text{CuSeO}_4$  was confirmed by UV-Visible spectrophotometer (Shimadzu UV- 2400). The colour intensity of synthesized As:  $\beta$ -CD IC/ $\text{CuSeO}_4$  was measured between the wavelengths 200 to 800 nm. The morphology and the size of the As:  $\beta$ -CD IC/ $\text{CuSeO}_4$  nanocomposite was predicted by a Carl Zeiss EVO 18 scanning electron microscope (SEM).

### 2.4 Photocatalytic activity

By examining how well the As: -CD IC/CuSeO<sub>4</sub> nanocomposite degraded dangerous MB and MO organic contaminants, researchers were able to determine its photocatalytic performance. For the photocatalytic activity, 40mg of nanocomposite was dispersed in 10 mg/L aqueous solutions of MB and MO organic pollutants and stirred by using a magnetic stirrer for 30 min to attain the adsorption equilibrium. After that, the photocatalytic process was carried out under UV-Visible light ( $\lambda = 254$  nm). During the photocatalytic process, a 5ml aliquot of the solution was collected at given time intervals and centrifuged to remove the suspension present in the solution. The samples were labelled. By using a UV-Vis spectrophotometer the absorbance of all the samples was recorded in the range of 200 to 900 nm. The percentage of photocatalytic degradation was estimated using the formula:

$$\text{MB and MO \%} = \frac{C_0 - C_t}{C_0} \times 100 \quad \text{----- 1}$$

Where  $C_0$  = initial concentration of dye;  $C_t$  = concentration of dye with time 't'.

## 2.5 Antimicrobial Activity

### 2.5.1 Microbial Culture

Six different bacterial strains—Streptococcus pyogenes, Enterococcus faecalis, Klebsiella pneumonia, Shigella flexneri, Staphylococcus aureus, and Escherichia coli—were employed in this investigation. All microbial isolates underwent a battery of morphological, physical, and traditional biochemical testing using the modified Kirby Bauer agar well diffusion method in accordance with the recommendations of the Clinical and Laboratory Standards Institute (CLSI).

### 2.5.2 Antimicrobial Assay of Nanocomposite

Agar well diffusion was used to perform an antimicrobial experiment on As:  $\beta$ -CD IC/CuSeO<sub>4</sub> nanocomposite in Muller Hinton Agar (MHA) plates. In order to adjust the turbidity to 0.5 McFarland standards, the test organisms were inoculated in Nutrient broth and incubated overnight at 37 °C, yielding a final inoculum of 1.5108 CFU/ml. The standard microbial culture broth was used to cultivate MHA plates. 50 mg/ml As:  $\beta$ -CD IC /CuSeO<sub>4</sub> was made in dimethyl sulfoxide (DMSO). Using a clean cork borer, three 6mm wells were made in the inoculated media (6 mm). 50, 75, and 100 ml of the positive control nanocomposite concentration were added to each well (DMSO). It was incubated for 18 to 24 h at 37 °C after being allowed to diffuse for about 30 min at room temperature. After incubation, plates were checked to see if a clear zone had formed around the well, signifying the tested compound's antimicrobial activity. The observed and mm-long zone of inhibition (ZOI) was assessed.

## 2.6 Antioxidant action (DPPH assay):

The antioxidant efficiency of As:  $\beta$ -CD IC/CuSeO<sub>4</sub> was determined using the DPPH (2, 2-diphenyl-1-picrylhydrazyl) assay to measure free radical scavenging activity [25]. The assay was run in triplicates. The As:  $\beta$ -CD IC/CuSeO<sub>4</sub> liquid sample was combined with 1 ml of DPPH (0.2 mM) and 1 ml of a control DPPH experiment without nanocomposites. These mixtures were stirred for three minutes at room temperature and without lighting. The reduction in the mixture's absorbance % after 20 min is then used to calculate the radical concentration. There was an excessive setting on the control. The change in absorbance at 517 nm was calculated. Ascorbic acid, a form of vitamin C, was used as a positive control. The equation was as follows:

$$\text{Radical Scavenging activity} = \frac{(\text{Control absorbance} - \text{Sample absorbance})}{\text{Control absorbance}} \times 100 \quad \text{-----}2$$

The absorbance in the absence of antioxidants is called control absorbance, whereas, the absorbance in the presence of antioxidants as As:  $\beta$ -CD IC/CuSeO<sub>4</sub> and Vitamin C is called sample absorbance.

### 3 Result and Discussion

#### 3.1 Structural analysis

X-ray diffraction (XRD) research was used to confirm that As:  $\beta$ -CD IC/CuSeO<sub>4</sub> is crystalline. The As:  $\beta$ -CD IC/CuSeO<sub>4</sub> nanocomposite as-synthesised XRD pattern is shown in Fig. 2. The As:  $\beta$ -CD IC/CuSeO<sub>4</sub> nanocomposite exhibits diffraction peaks that can be indexed to the (111), (002), (200), (040), (211), (140), (231) and (133) planes at 27.76 °, 29.66 °, 41.32 °, 43.64 °, 46.30 °, 49.72 °, and 61.2 °. The composite's intensities closely matched those of the industry-standard JCPDS # 17-0842. No recognisable impurity peak is found, indicating that pure As:  $\beta$ -CD IC/CuSeO<sub>4</sub> was formed. The calculated average lattice constants, which are equal to 5.099 °A, 9.390 °A, and 7.005 °A, are in line with previously published data and typical JCPDS values. Most of the major peaks are sharp, which indicates the high crystallinity of the As:  $\beta$ -CD IC/CuSeO<sub>4</sub> nanocomposite. The average size of the nanocomposite was calculated by using Debye–Scherer equation as shown below in Eq. (3)

$$D = \frac{n\lambda}{\beta \cos\theta} \dots \dots \dots 3$$

where n is the dimensionless form factor (0.9),  $\lambda$  is the wavelength of the incident X-ray (= 1.54 Å), D is the nanoparticle's crystalline size,  $\theta$  is the angle of diffraction,  $\beta$  is the full width at half maximum (FWHM) of the diffraction peak. The average size of the composite is calculated to be 10 nm. From the XRD pattern, we conclude that there are two different angle peaks are obtained;

those are low angle peaks and wide-angle peaks. The low-angle peak is obtained due to interlayer arrangements of atoms in the lattice and the wide-angle peak is due to the intercrystalline of the composite. The XRD peaks are fitting by using the Lorentzian expression.

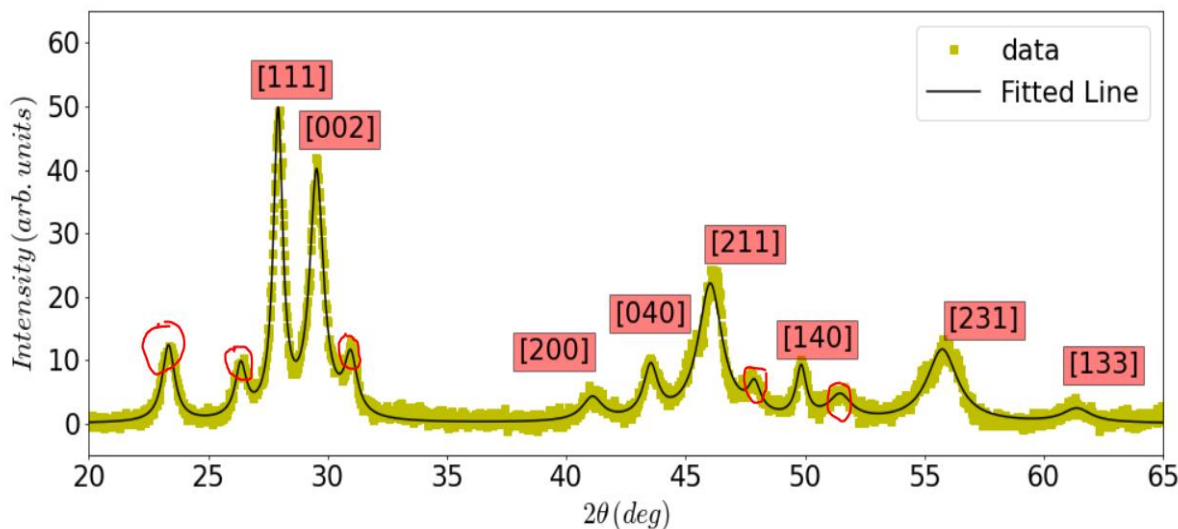


Fig.2.XRD patterns of as-synthesized As:  $\beta$ -CD IC/CuSeO<sub>4</sub>nanoparticles.

### 3.2 SEM analysis

The surface morphology of as-prepared As:  $\beta$ -CD IC/CuSeO<sub>4</sub> was investigated by using scanning electron microscopy (SEM). Fig. 3 (a-b) shows the SEM image of the As:  $\beta$ -CD IC/CuSeO<sub>4</sub> nanocomposite. On the surface of the Cu beads, it can be seen from the microscope (Fig. 3b) that there are a lot of Se particles that resemble needles. The agglomerated morphology of the composite is due to the presence of capping agents which were used for the preparation of nanocomposite [26]. By means of Van der Waals forces, the As:  $\beta$ -CD IC/CuSeO<sub>4</sub> nanocomposite was anchored to the  $\beta$ -CD surface [27]. The voids and gaps between the nanocomposites are clearly noticed in Fig. 3a. These small pores between the particles in nanocomposite potentially help to enhance the photocatalytic activity of As:  $\beta$ -CD IC/CuSeO<sub>4</sub>

nanocomposite due to the charge transfer and electrolyte permeation during the reduction process.

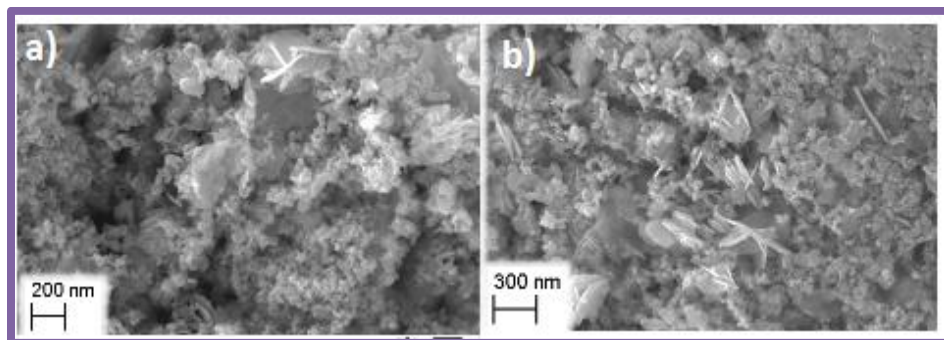


Fig.3 SEM image of as-prepared As:  $\beta$ -CD IC/ $\text{CuSeO}_4$

### 3.3 EDX analysis:

Energy-dispersive X-ray spectroscopy (EDX) was used to predict the elemental composition present in the sample. EDX Spectrum of As:  $\beta$ -CD IC/ $\text{CuSeO}_4$  consisted of Copper, Selenium and Oxygen only, which confirms the purity of the composite and no other impurities were present in the as-prepared composite was shown in Fig. 4. The atomic weight percentage of the Cu, Se and O elements as illustrated in Table.1. In order to further support the development of the As:  $\beta$ -CD IC/ $\text{CuSeO}_4$  nanocomposite, elemental mapping analysis was also performed, and the distribution of Cu and Se on the  $\beta$ -CD surface is shown in Fig 5.

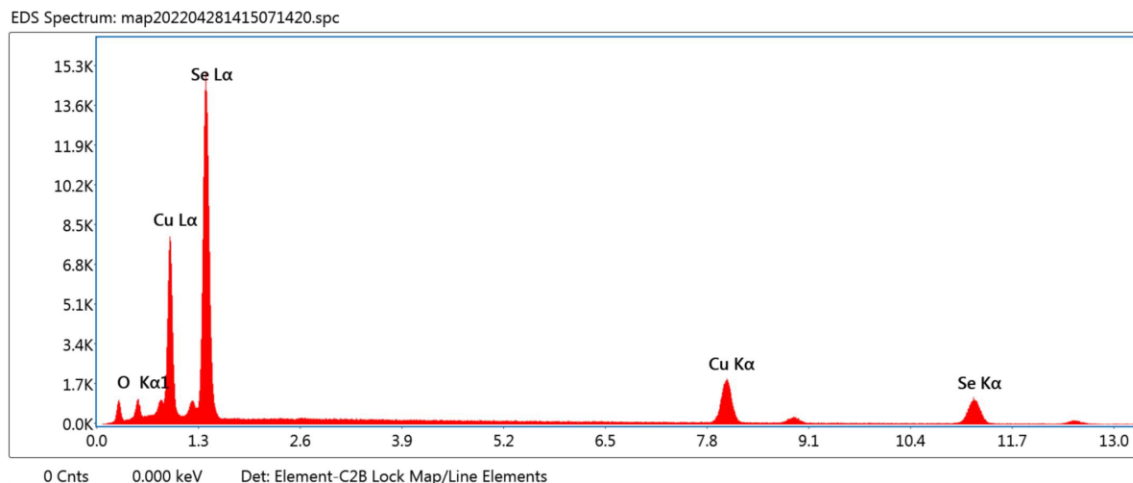


Fig.4. EDX spectrum of  $\text{CuSeO}_4$  nanocomposite

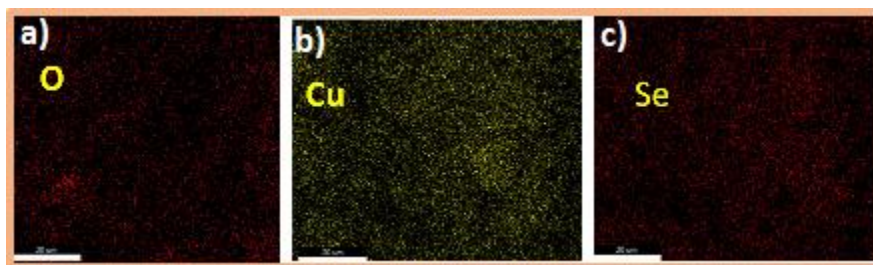


Fig 5. The elemental mapping of  $\text{CuSeO}_4$  nanocomposite

**Table 1**

Weight percentage of elements in mapping analysis.

Element	Weight %	Atomic %	Error %	Kratio
O K	4.2	16.9	10.8	0.0119
Cu K	25.7	26.0	3.0	0.2884
Se K	70.2	57.2	3.7	0.6669

### 3.4 Optical Property

The optical property and light absorption range of As:  $\beta$ -CD IC/CuSeO<sub>4</sub> was monitored by DRS – UV Spectroscopy. DRS-UV spectrum is one of the most important tools for constructing the energy band diagram. As seen in Fig. 6, the pure As:  $\beta$ -CD IC/CuSeO<sub>4</sub> exhibits a good absorbance edge at 380 nm (UV- Region) and the absorption is gradually increasing beyond the critical wavelength, it reaches a maximum and it shows a plateau region till 850 nm.

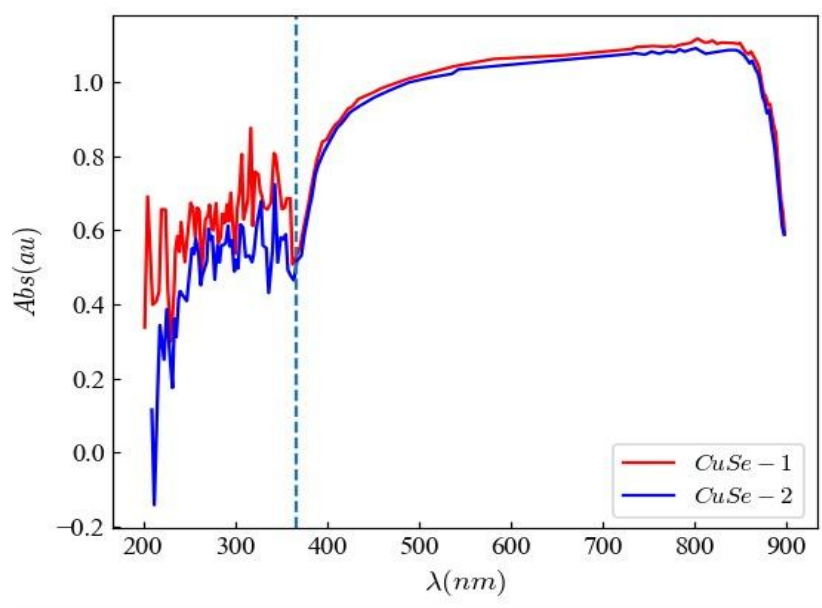


Fig.6. DRS-UV spectrum of As:  $\beta$ -CD IC/CuSeO<sub>4</sub>

### 3.5. Photodegradation of organic pollutants (MB and MO)

The photocatalytic action of as-prepared As:  $\beta$ -CD IC/CuSeO<sub>4</sub> nanocomposite was predicted by the degradation of MB and MO dye under the illumination of UV light Fig7 (a-b). The As:  $\beta$ -CD IC/CuSeO<sub>4</sub> catalyst degrades the maximum concentration of the MB and MO dye within 80 and 90 min. The As:  $\beta$ -CD IC/CuSeO<sub>4</sub> catalyst exhibits 68.97 and 61.11% of degradation efficiency against MB and MO dye. The UV-Visible spectra of the MB and MO degradation stand nearby 650 and 460 nm which are correlated to many kinds of literature which

were shown in Table 2. Finally, the As:  $\beta$ -CD IC/ $\text{CuSeO}_4$  shows superior catalytic performance may owing to the prevention of electron-hole pair recombination.

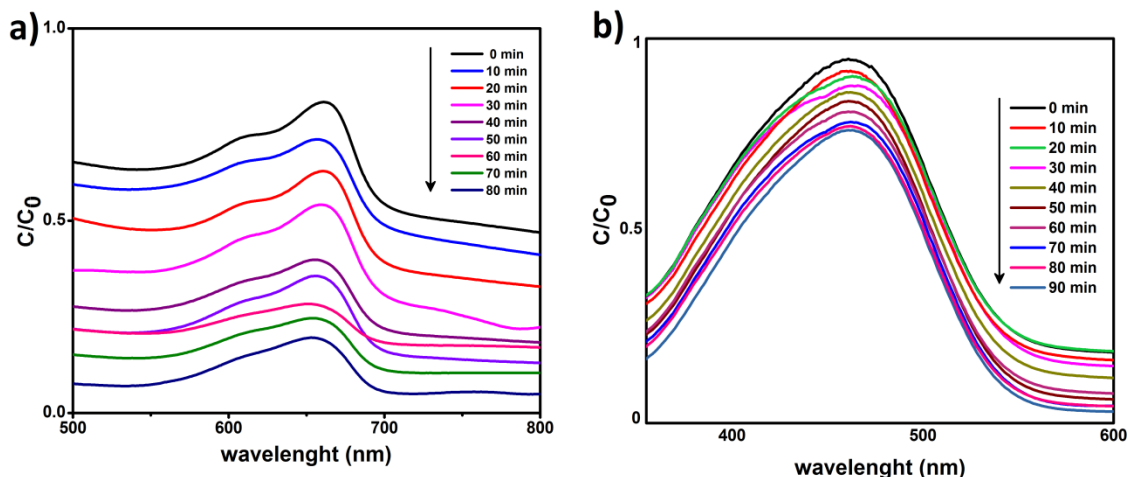


Fig. 7. Absorption spectrum of photodegradation of a) MB and b) MO dye under the illumination of UV-light.

**Table 2**

Comparative account of photocatalytic activity of as prepared As:  $\beta$ -CD IC/ $\text{CuSeO}_4$  nanocomposite with various photocatalyst previously reported for degradation of organic pollutant

S.No	Catalyst	Wight of catalyst (g/L)	Organic Pollutant	Irradiation source	% of degradation	Degradation time (min)	Reference
1.	As: $\beta$ -CD IC/ $\text{CuSeO}_4$	0.04	MB & MO	UV light	68.97 % & 61.11%	80 & 90	This work
2.	GO/NiO/ $\beta$ -CD	0.1 -0.8	MB & MV	Solar light	90 & 69.54	120	28

3.	Selenide - chitosan	0.1 – 0.5	Alizarin Red S	Solar light	86.7	180	29
4.	CeVO <sub>4</sub>	0.0005	MO	UV light	75	60	30
5.	CeVO <sub>4</sub>	0.05	MB	UV light	80	300	31

### 3.6 Antioxidant test

Oxidative stress and other health issues are brought on by free radicals [32]. A prevalent hazardous free radical called DPPH has had negative consequences on people's health [33]. The antioxidant property of As:  $\beta$ -CD IC/CuSeO<sub>4</sub> may be due to the donation of electrons from the highly dense oxygen atom in this nanocomposite to the odd electron on the nitrogen atom in the DPPH molecule, which causes a decrease in the intensity of the  $n \rightarrow \pi^*$  transition at 517 nm and the disappearance of DPPH's violet colour. In this study, as the concentration of As:  $\beta$ -CD IC/CuSeO<sub>4</sub> range from 12.5 to 50 M, the scavenging percentage of DPPH grew exponentially from 14.37 to 49.52%. (Fig.8a-b). Here, we used Vitamin C as a positive standard and achieved, respectively, 15.63, 24.64, 37.51, and 54.38% of DPPH scavenging at concentrations of 12.5 to 50 M, which are equivalent to As:  $\beta$ -CD IC/CuSeO<sub>4</sub> (Fig. 8a-b). As:  $\beta$ -CD IC/CuSeO<sub>4</sub> was subsequently demonstrated to have acceptable antioxidant activity against DPPH and is anticipated to be employed to neutralise additional free radicals [34,35].

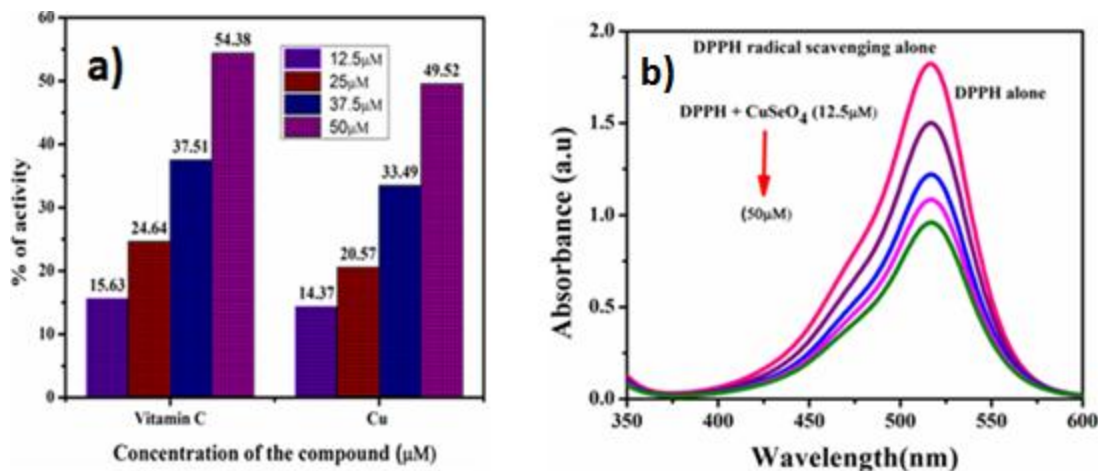


Fig.8. Antioxidant efficiency of As:  $\beta$ -CD IC/CuSeO<sub>4</sub> nanocomposite and Vitamin C (Positive Control) against DPPH.

### 3.7 Antibacterial study

Numerous medicinal uses have made use of the well-known inhibitory capabilities of Cu and Se nanoparticles, most notably the inhibition of gram-positive and gram-negative bacterial strains. Additionally, As: $\beta$ -CD IC/CuSeO<sub>4</sub> was tested for its antimicrobial efficacy against various gram-positive and gram-negative bacteria, including *Streptococcus pyogenes*, *Staphylococcus aureus*, and *Enterococcus faecalis* [36]. Gram-negative bacteria tested included *Escherichia coli*, *Klebsiella pneumonia*, and *Shigella flexneri*. The outcomes showed that As: $\beta$ -CD IC/CuSeO<sub>4</sub> is an effective antibacterial agent against *Enterococcus faecalis* since it completely stopped the bacteria's growth at a high concentration (100 g/ml) and produced an inhibition zone that measured 18 mm. Table 3 lists the findings against several bacteria that were acquired. Because of this, As: $\beta$ -CD IC/CuSeO<sub>4</sub> can be used as an effective antibacterial material to disinfect wastewater from *Enterococcus faecalis*.

**Table 3**

Diameter of zones of inhibition (mm) of sample Cu@Se nanocomposite against microorganisms

S.No.	Name of microorganism	Nanocomposite Concentration ( $\mu\text{g/ml}$ )			
		50	75	100	DMSO (100 $\mu\text{l}$ )
1.	<i>Streptococcus pyogenes</i>	8mm	8mm	10mm	No Zone
2.	<i>Enterococcus faecalis</i>	10mm	10mm	18mm	No Zone
3.	<i>Klebsiella pneumonia</i>	No Zone	8mm	10mm	No Zone
4.	<i>Shigella flexneri</i>	No Zone	8mm	8mm	No Zone
5.	<i>Staphylococcus aureus</i>	8mm	10mm	15mm	No Zone
6.	<i>Escherichia coli. A</i>	10mm	10mm	12mm	No Zone

#### 4 Conclusion

In summary, As: $\beta$ -CD IC/CuSeO<sub>4</sub> nanocomposite was successfully prepared by a simple, eco-friendly chemical precipitation method. The characterisation of As: $\beta$ -CD IC/CuSeO<sub>4</sub> composite was performed by various spectroscopic and analytical techniques. The composite was further used to design the catalytic platform for the degradation of MB and MO dyes. The results obtained from photocatalytic experiments confirmed the excellent ability of biosynthesized nanocomposites in the degradation of MB and MO organic dyes with 68.97 and 61.11% efficiencies respectively. Furthermore, the antioxidant and antimicrobial activity of As  $\beta$ -CD IC/CuSeO<sub>4</sub> composite was also carried out. The results suggest that As: $\beta$ -CD IC/CuSeO<sub>4</sub> composite has superior antioxidant and antimicrobial activity. Finally, this investigation showed

that the As: $\beta$ -CD IC/CuSeO<sub>4</sub> nanocomposite could be a better candidate for the wastewater degradation of MB and MO dyes.

## Reference

1. Fang X, Zhai T, Gautam U K, Li L, Wu L, Bando Y and Golberg D 2011 ZnS nanostructures: from synthesis to applications *Prog. Mater. Sci.* **56** 175 – 287
2. Liu H, Zhang Z, Hu L, Gao N, Sang L, Liao M, Ma R, Xu F and Fang X 2014 New UV – A photodetector based on individual potassium niobite nanowires with high performance *Adv. Opt.Mater.* **2** 771-8
3. Hamann S, Brunken H, Salomon S, Meyer R, Savan A and Ludwig A 2013 Synthesis of Au microwires by selective oxidation of Au-W thin-film composition spreads *Sci. Technol. Adv. Mater.* **14** 015003
4. Fang X, Hu L, Huo K, Gao B, Zhao L, Liao M, Chu P K, Bando Y and Golberg D 2011 New ultraviolet photodetector based on individual Nb<sub>2</sub>O<sub>5</sub> nanobelts, *Adv. Funct. Matr.* **21** 3907-15
5. A. Azadbakht, M. Roushani, A.R. Abbasi, S. Menati , Z. Derikvand, 2016 A label – free aptasensor based on polyethyleneimine wrapped carbon nanotubes in situ formed gold nanoparticles as signal probe for highly sensitive detection of dopamine. *Mater. Sci. Eng. C* **68** 585 – 593
6. G.S. Anand, A. Sivanesan, M.R. Benzigar, G. Singh, A.I. Gopalan, A.V. Baskar, H. Ilbeygi, K. Ramadass, V. Kambala, A. Vinu, Recent progress on the sensing of pathogenic bacteria using advanced nanostructures, *Bull. Chem. Soc. Jpn.* **92** (2019) 216–244.
7. Q. Ji, I. Honma, S.M. Paek, M. Akada, J.P. Hill, A. Vinu, K. Ariga, Layer-by-layer films of graphene and ionic liquids for highly selective gas sensing, *Angew. Chem. Int. Ed.* **49** (2010) 9737–9739.
8. N. Joshi, T. Hayasaka, Y. Liu, H. Liu<sup>1</sup>, O.N. Oliveira Jr., L. Lin, A review on chemiresistive room temperature gas sensors based on metal oxide nanostructures, graphene and 2D transition metal dichalcogenides, *Micro* **185** (2018) 213.
9. C.N.R. Rao, K. Pramoda, Borocarbonitrides, B<sub>x</sub>C<sub>y</sub>N<sub>z</sub>, 2D nanocomposites with novel properties, *Bull. Chem. Soc. Jpn.* **92** (2019) 441–468.
10. L. Wang, A. Wu, G. Wei, Graphene-based aptasensors: from molecule–interface interactions to sensor design and biomedical diagnostics, *Analyst* **143** (2018) 1526–1543.

11. Sinha S K, Srivastava C, Sampath S and Chattopadhyay K 2015 Tunability of monodispersed intermetallic AuCu nanoparticles through understanding of reaction pathways *RSC Adv.* **5** 4389–95
12. Hong X, Wang D, Yu R, Yan H, Sun Y, He L, Niu Z, Peng Q and Li Y 2011 Ultrathin Au–Ag bimetallic nanowires with coulomb blockade effects *Chem. Commun.* **47** 5160–2
13. Koenigsman C, Santulli A C, Gong K, Vukmirovic M B, Zhou W-P, Sutter E, Wong S S and Adzic R R 2011
14. Enhanced electrocatalytic performance of processed, ultrathin, supported Pd–Pt core–shell nanowire catalysts for the oxygen reduction reaction *J. Am. Chem. Soc.* **133** 9783–95
15. Zhang H, Jin M, Wang J, Li W, Camargo P H C, Kim M J, Yang D, Xie Z and Xia Y 2011 Synthesis of Pd–Pt bimetallic nanocrystals with a concave structure through a bromide-induced galvanic replacement reaction *J. Am. Chem. Soc.* **133** 6078–89
16. Singh N, Dogan E, Karaman I and Arróyave R 2011 Effect of configurational order on the magnetic characteristics of Co– Ni–Ga ferromagnetic shape memory alloys *Phys. Rev. B* **84** 184201
17. Liu Z, Jackson G S and Eichhorn B W 2010 PtSn intermetallic, core–shell, and alloy nanoparticles as CO-tolerant electrocatalysts for H<sub>2</sub> oxidation *Angew. Chem. Int. Ed.* **49** 3173–6
18. Wang D, Xin H L, Hovden R, Wang H, Yu Y, Muller D A, DiSalvo F J and Abruña H D 2013 Structurally ordered intermetallic platinum–cobalt core–shell nanoparticles with enhanced activity and stability as oxygen reduction electrocatalysts *Nat. Mater.* **12** 81–7
19. Kang Y, Pyo J B, Ye X, Gordon T R and Murray C B 2012 Synthesis, shape control, and methanol electro-oxidation properties of Pt–Zn alloy and Pt<sub>3</sub>Zn intermetallic nanocrystals *ACS Nano* **6** 5642–7
20. Deevi S C and Sikka V K 1996 Nickel and iron aluminides: *an overview on properties, processing, and applications* *Intermetallics* **4** 357–75
21. Vedantam T S, Liu J P, Zeng H and Sun S Thermal stability of self-assembled FePt nanoparticles 2003 *J. Appl. Phys.* **93** 7184–6
22. V. Dusastre, B. Omar, I. P. Parkin and G. A. Shaw, *J.Chem.Soc., Dalton Trans*, 1997, 3505.
23. V. M. Garcia, P. K. Nair and M. T. S. Nair, *J. Cryst. Growth*, 1999, 203, 113.
24. Mohamed Hosny, Manal Fawzy, Abdelazeem S.Eltaweil. "Green synthesis of bimetallic Ag/ZnO@Biohar nanocomposite for photocatalytic degradation of tetracycline, antibacterial and antioxidant activities", *Scientific Reports*, 2022.
25. Javier Suárez-Cerda, Heriberto Espinoza-Gómez, Gabriel Alonso-Núñez, Ignacio A. Rivero et al. "A green synthesis of copper nanoparticles using native cyclodextrins as

- stabilizing agents", Journal of Saudi Chemical Society, 2017.
26. Vahid Ameri, Mohammad Eghbali – Arani, Saeid Pourmasoud, New route for the preparation of cerium vanadate nanoparticles with different morphology and investigation of optical and photocatalytic properties. *J.Mater.Sci:Mater.Electron*, 2017.
  27. Ranjana Dewangan, Ayesha Hashmi, Anupama Asthana, Ajaya K.Singh, Degradation of methylene blue and methyl violet using graphene oxide/NiO/ $\beta$ -cyclodextrin nanocomposites as photocatalyst. *International Journal of Environmental and analytical chemistry*. **102**, 2020.
  28. Nisar Ali, Shehzad Ahmad, Adnan Khan, Saraf Khan, Muhammad Bilal, Salah Ud Din, Nauman Ali, Hafiz.N. Iqbal. Hammad Khan, Selenide-chitosan as High-performance Nanophotocatalyst for Accelerated Degradation of Pollutants. *Chemistry. An Asian Journal*, 2020.
  29. Mohammadreza Mosieh, Afsane Mahinpour, Sonochemical synthesis and characterisation of cerium vanadate nanoparticles and investigation of its photocatalyst application. *J. Mater. Sci: Mater Electron*, 2016.
  30. K. Leeladevi, M. Arunpandian, J. Vinoth Kumar, T. Chellapandi, M. Thiruppathi, G. Madhumitha, Jeong-Won Lee, E.R. Nagarajan a, Fabrication of 3D pebble-like CeVO<sub>4</sub>/g-C<sub>3</sub>N<sub>4</sub> nanocomposite: A visiblelight-driven photocatalyst for mitigation of organic pollutants, *Diamond & Related Materials*. **116**, 2021.
  31. Hosny, M. & Fawzy, M. Instantaneous phytosynthesis of gold nanoparticles via *Persicaria salicifolia* leaf extract, and their medical applications. *Adv. Powder Technol.*
  32. Soren, S. et al. Evaluation of antibacterial and antioxidant potential of the zinc oxide nanoparticles synthesized by aqueous and polyol method. *Microb. Pathog.* **119**, 145–151, 2018.
  33. Rajeswari, R. & Prabu, H. G. Palladium–decorated reduced graphene oxide/zinc oxide nanocomposite for enhanced antimicrobial, antioxidant and cytotoxicity activities. *Process. Biochem.* **93**, 36–47 (2020).
  34. Ali, A. et al. Zinc impregnated cellulose nanocomposites: Synthesis, characterization and applications. *J. Phys. Chem. Solids* **98**, 174–182, 2016.
  35. K.Kaviyarasu, A.Ayeshamariam, E. Manikandan, J. Kennedy, R. Ladchumananandasivam, U.U. Gomes, M. Jayachandran, M. Maaza, Solution processing

of CuSe quantum dots: Photocatalytic activity under RhB for UV and visible-light solar irradiation, *Mater. Sci. Eng. B* **210**, 2016, 1–9.

36. Abdelazeem S. Eltaweli, Manal Fawzy, Mohamed Hosny, Eman M. Abd El-Monaem, Tamer M. Tamer, Ahmed M. Omer: Green synthesis of platinum nanoparticles using *Atriplex halimus* leaves for potential antimicrobial, antioxidant, and catalytic applications, *Arabian Journal of Chemistry*, 2022.